Iranian Journal of Oil & Gas Science and Technology, Vol. 8 (2019), No. 3, pp. 01-17
http://ijogst.put.ac.ir

An Experimental Study on the Operating Parameters of Ultrasound-assisted Oxidative Desulfurization

Seyede Leila Ebrahimi[1], Mohammad Reza Khosravi-Nikou[*2], and Seyed Hassan Hashemabadi[3]

[1] Ph.D. Candidate, Gas Engineering Department, Petroleum University of Technology (PUT), Ahwaz, Iran
[2] Associate Professor, Gas Engineering Department, Petroleum University of Technology (PUT), Ahwaz, Iran
3 Professor, School of Chemical Engineering, Iran University of Science and Technology, Tehran, Iran

Received: February 06, 2019; *revised*: February 15, 2019; *accepted*: February 25, 2019

Abstract

In this research, the effects of important parameters, including the molar ratio of acetic acid to sulfur(S) , sonication time, temperature, and hydrogen the molar ratio of peroxide to sulfur on the performance of ultrasound-assisted oxidative desulfurization were studied using the response surface method (RSM). To this end, a model fuel containing n-decane and dibenzothiophene at a concentration of 1000 ppm was used. It was found out that the temperature and acetic acid/S molar ratio were the most influencing parameters affecting the conversion of sulfur compound. The synergistic effects of the parameters were also investigated, and it was discovered that the maximum conversion of dibenzothiophene reached 98.59% when H_2O_2/S, acetic acid/S, temperature, and sonication time were set to 167, 330, 80 °C, and 30 min respectively. Finally, the apparent kinetics of dibenzothiophene oxidation and the activation energy of reaction were presented.

Keywords: Ultrasound-assisted Oxidative Desulfurization (UAOD), Liquid Hydrocarbon Fuel, Dibenzothiophene, Model Fuel

1. Introduction

Generally, sulfur-containing compounds are transferred to the final products as the main contaminants during refining hydrocarbon fuels. In this way, because of the depletion of hydrocarbon sources, the level of these contaminants increases in raw materials; thus, they are known to be one of the most important environmental issues threatening human beings. In this regard, fuels with high levels of sulfur-containing compounds produce sulfur dioxide and particulate substances after burning in the engines of vehicles. Moreover, such compounds poison catalysts in catalytic converters, which may lead to the corrosion of combustion chamber and inner parts. As a consequence, stringent environmental regulations have been recognized to reduce the sulfur levels in hydrocarbon petroleum products. The effect of these strict regulations can also introduce new challenges on the operation conditions and economical dimension of refining processes. Therefore, to make the sulfur level in final products acceptable to be used in automotive engines, novel processes have been examined and studied (Dai et al., 2010; Jalali and Sobati, 2017; Margeta et al., 2016; Rahimi et al., 2017; Rashidi et al., 2015; Rashidi et al., 2015; Te et al., 2001). Hydrodesulfurization (HDS) is a kind of industrial technology which is

* Corresponding author:
Email: mr.khosravi@put.ac.ir

commonly employed to reduce sulfur compounds in petroleum feedstocks. In this technology, hydrogen is used to react with sulfur molecules in the existing compounds. However, it requires a high temperature (up to 400 °C), a high pressure (up to 100 atm), and expensive metallic catalysts such as NiMo and CoMo (Mohammadian et al., 2017). Previous researches have indicated that there is a limitation to HDS process since it removes aromatic sulfur containing compounds such as thiophenes, benzothiophenes (BT's), and dibenzothiophenes (DBT's); they are known as a main portion of sulfur sources in diesel and gasoline products. To overcome the limitations of HDS process, a number of methods such as adsorptive desulfurization (ADS), extractive desulfurization (EDS), biodesulfurization (BDS), oxidative desulfurization (ODS), and photo-oxidative desulfurization (phODS) have so far been introduced (Ahmadi et al., 2017; Ja'fari et al., 2018). Among these newly-established technologies, ODS has been known to be a promising method due to using mild conditions, which reduce the operating costs. This process can convert sulfur compounds into more polar compounds like sulfoxide and sulfone compounds, which can be removed through extraction or adsorption (Sasanipour et al., 2017). To this end, several reagents such as H_2O_2-formic acid, H_2O_2-acetic acid, hydroperoxide-MoO_3-Al_2O_3, ozone, nitric acid, H_2O_2-photocatalyst, H_2O_2-phase transfer catalyst, and H_2O_2-inorganic solid acid have been introduced as the oxidation system (Ahmed et al., 2015; Akbari et al., 2015; Bachmann et al., 2014; Ja'fari et al., 2018; Ja'fari et al., 2016; Mohammadian et al., 2017; Mohammadian et al., 2017; Sahragard et al., 2017). Extraction and adsorption can be utilized after the oxidization of sulfur-containing compounds. Along with the advantages of ODS process, some limitations, including H_2O_2 decomposition, sonication time, and the low efficiency of sulfur removal also exist. Therefore, in order to overcome these deficiencies in the ODS process, previous researchers have recommended using ultrasonic irradiation. It is capable of enhancing the reaction rate mainly due to the formation, growth, and implosive collapse of bubbles in a liquid phase. Meanwhile, this phenomenon creates hot spots having a temperature of about 5000 K and a pressure of about 1000 atm at the speed of 10^{10} k/s. Such microstreaming with extreme local conditions facilitates the generation of active intermediates which, in effect, can enhance the reaction rate. Some studies report using ultrasonic waves in different areas of petroleum industries (Duarte et al., 2011). Some others have explored the ultrasound-assisted oxidative desulfurization (UAOD) with different systems of oxidants (Margeta et al., 2016). Past researches have concluded that the UAOD process will be the only method used for desulfurization in the future, which can produce low and ultra-low sulfur fuels. However, some aspects of the UAOD such as scale-up and integration with upstream in refineries are yet to be investigated. Although using ultrasonic waves for the improvement of mixing efficiency has been considered by a bulk of researches, many problems still exist in the UAOD process (Shayegan et al., 2013). The implosion of bubbles producing active intermediates such as alkyl radical and hydrogen radical (Tang et al., 2013) has been reported to increase the rate of heat and mass transport (Parvizian et al., 2012; Parvizianet al., 2012). It leads to micro-streaming, microjet, micro turbulence, and shock waves (Ja'fari et al., 2018). In addition, ultrasound power can be used in other fields because it has a number of advantages such as facilitating the synthesis of nano zero valent iron particles (NZVI) (Jamei et al., 2013; Jamei et al., 2014). Hence, it can also be used in waste-water treatment and soil remediation. These chemical and physical effects can make the selectivity of the process better and can enhance the reaction rate and efficiency of the UAOD. In this way, the sonication of the reaction medium is considered to be a favorable method for the oxidative desulfurization of liquid fuels (Wu et al., 2010).

The efficiency of the UAOD process depends on a large number of factors such as sonication time, temperature, the type and amount of oxidant, the type and amount of catalyst, the type and amount of phase transfer agent, the type and initial concentration of sulfur containing compounds, and ultrasound amplitude. In this context, Ebrahimi et al. showed that the efficiency of desulfurization is related to reactor material, probe diameter, and reagent amount (Ebrahimi et al., 2018). In addition, Khodaei et

al. (Khodaei et al., 2016a) examined sulfur removal from kerosene using the Box–Behnken design (BBD). They reported that a sulfur removal of 95.46% was achieved under optimal oxidation conditions after a sonication time of 10.5 min. Similarly, Karami et al. (Karami et al., 2017) applied the ultrasound-assisted oxidation to a model fuel (benzothiophene in toluene) using BBD design and explored the effects of several parameters, including the molar ratio of formic acid to sulfur (Acid/S), the molar ratio of hydrogen peroxide to sulfur (O/S), and temperature on DBT conversion. Their findings revealed that one of the most important parameters was the molar ratio of formic acid to sulfur. Furthermore, Khodaei et al. (Khodaei et al., 2016b) studied four factors using RSM. They indicated that, in an optimum condition, a conversion of 97.5% was obtained for the oxidation of DBT. Lu et al. (Lu et al., 2014) explored the effects of agitation speed (7400 to 14,000 rpm), temperature (50–70 °C), and sonication time (10–30 min) on the sulfur conversion using the Box–Behnken design. They compared their results with ultrasound-assisted oxidative desulfurization, and the same level of desulfurization was achieved using both systems.

The present study, however, sought to investigate ultrasound-assisted oxidative desulfurization by applying response surface methodology and employing a central composite design (CCD). To this end, we study the effects of different factors, including sonication time, temperature, the molar ratio of oxidant to sulfur, and the molar ratio of acetic acid to sulfur. Finally, a reaction kinetic model was presented for the oxidation of DBT in n-decane as the model fuel.

2. Experimental

2.1. Reagent and materials

Dibenzothiophene ($C_{12}H_8S$, purity ≥98%, Merck) was purchased from Merck Millipore, Germany. Glacial acetic acid (CH_3COOH, purity≥99.7%), H_2O_2 (34.5%), and n-decane (98.0%) were supplied by Samchun Company. All the materials were of analytical grade and used as they were received without further purification.

2.2. Analysis method

The sulfur content of the treated model fuel was measured by gas chromatography (YL 6100GC, Younglin, Korea), which was equipped with a TRB-5 capillary column (length: 30 m, internal diameter: 0.320 mm, and film thickness: 1 µm) and a flame ionized detector (FID) utilizing helium as the carrier of gas.

2.3. Experimental procedure

In order to irradiate ultrasound waves, UIP1000hd provided by Hielscher, Germany was employed. Its processor can generate waves at a frequency of 20 kHz and at a maximum power of 1000W. In addition, the modeled fuel, which was the representative of a liquid fuel, was prepared using n-decane and dibenzothiophene (DBT). Then, 0.73 gr of DBT was dissolved in 1 liter of n-decane to obtain the optimal DBT solution of at a concentration of 1000 ppm.

For each experiment, a cylindrical jacketed reactor was made from Pyrex glass and was equipped with a condenser and a thermometer. Additionally, the temperature of the reactor was controlled by passing cool water through its jacket. In each of the tests, an appropriate volume of the model fuel was added to the reactor, and the sonotrode was dipped into the reaction mixture in a way that a length of 7 mm was submerged by the model fuel. Next, hydrogen peroxide and acetic acid were mixed in another vessel and were then added to the reactor. Afterwards, the sonication process started for a pre-defined time. Then, the sonication was stopped, and the reaction medium was transferred into a separator funnel

to be manually shaken for 3 min. The separator funnel was then rested for a certain time to let the phases separate. After 8 min, the aqueous phase was separated from the organic phase, and a sample was withdrawn from the organic phase in order to determine the final sulfur content of the fuel. The whole process is presented in Figure 1. These experiments were repeated twice with an average standard deviation of 1.4.

a)

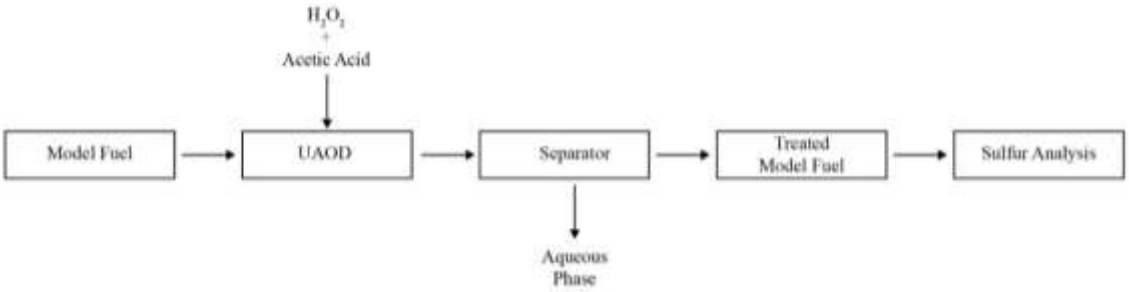

b)

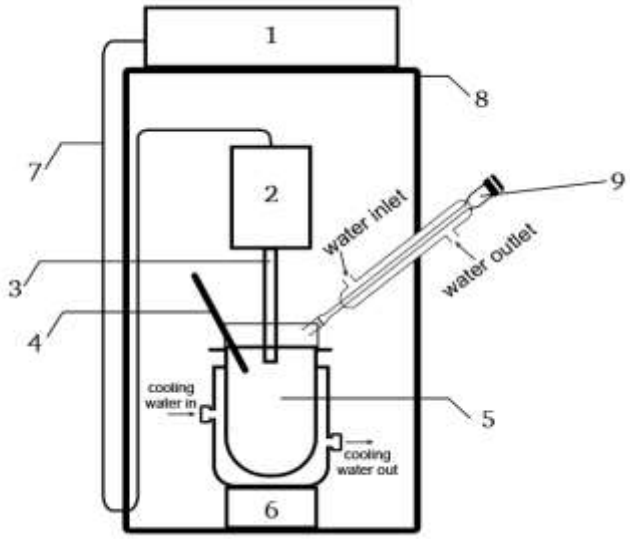

Figure 1

a) A graphical schematic of the UAOD procedure and b) The experimental setup: 1) generator, 2) ultrasonic transducer, 3) sonotrode,4) thermometer, 5) reactor vessel, 6) lift, 7) wire 8), and sound protection box.

2.4. Experimental design

To investigate the effects of the four important parameters on DBT conversion, response surface methodology was utilized on the basis of a central composite design (CCD). In this context, the effects of sonication time, temperature, the molar ratio of hydrogen peroxide to sulfur, and the molar ratio of acetic acid to sulfur were studied. It is worth noting that, in all the experiments, the other parameters such as power input (800 W), DBT initial concentration (1000 ppm), the ratio of probe diameter to reactor diameter (0.27), and the ratio of probe immersion length to liquid fuel height (0.245) were kept constant. Finally, design expert (Version 10) was used to implement the experimental design and data analysis.

The experimental range and levels of parameters are listed in Table 1. According to the central composite design, thirty experiments are required for the examination of the individual effects of each variable. DBT conversion as a response variable was calculated using the following equation:

$$Conversion\ of\ DBT\ (\%) = \frac{S_0 - S}{S_0} \times 100 \quad (1)$$

where, S_0 and S are the initial and final concentration of DBT in each test respectively. The correlation between DBT conversion and investigated parameters and their interactions can be represented in the following form:

$$Y = \beta_0 + \sum_{i=A}^{E} \beta_i x_i + \sum_{i=A}^{E} \sum_{i \neq j=A}^{E} \beta_{ij} x_i x_j + \sum_{i=A}^{E} \beta_{ii} x_{ii}^2 + \varepsilon \quad (2)$$

where, Y is DBT conversion, and β_0 is the intercept; β_i, β_{ii} , and β_{ij} are the parameters of linear effects, quadratic effects, and interaction effects respectively. Here, x_i and x_j indicate the coded levels for the independent variables, and ε is the unanticipated error.

Table 1

The experimental range and levels of process variables for the central composite design.

Independent variable	Range and levels		
	-1	0	1
H_2O_2/S molar ratio (mol/mol): *A*	167	334	501
Acetic acid/S molar ratio (mol/mol): *B*	110	220	330
Temperature (°C): *C*	50	65	80
Sonication time (min): *D*	10	20	30

3. Results and discussion

3.1. Statistical analysis

The present research studied the effects of four parameters, namely sonication time, temperature, the molar ratio of H_2O_2 to sulfur, and the molar ratio of acetic acid to sulfur, on DBT conversion of a model fuel. To this end, it utilized an experimental design via applying central composite design. The runs and the response values for each test are presented in Table 2.

Table 2

The experimental runs and the corresponding DBT conversions.

Run	Factor 1 ***A*: H_2O_2/S molar ratio (mol/mol)**	Factor 2 ***B*: Acetic acid /S molar ratio (mol/mol)**	Factor 3 ***C*: Temperature (°C)**	Factor 4 ***D*: Sonication time (min)**	Response 1 **DBT conversion (%)**
1	167	110	50	10	31.17
2	334	220	65	10	60.37

Run	Factor 1 *A*: H_2O_2/S molar ratio (mol/mol)	Factor 2 *B*: Acetic acid /S molar ratio (mol/mol)	Factor 3 *C*: Temperature (°C)	Factor 4 *D*: Sonication time (min)	Response 1 DBT conversion (%)
3	167	110	80	10	39.88
4	334	220	65	20	88.79
5	167	330	80	30	98.59
6	167	330	50	10	51.62
7	501	330	50	30	59.54
8	334	110	65	20	50.13
9	167	220	65	20	81.04
10	334	220	65	20	83.89
11	334	220	65	30	93.32
12	501	330	50	10	37.02
13	501	110	50	10	9.21
14	501	330	80	30	96.62
15	501	110	80	10	30.2
16	334	220	65	20	83.98
17	501	330	80	10	80.55
18	167	110	80	30	76.45
19	501	220	65	20	60.41
20	167	330	50	30	62.6
21	167	330	80	10	71.32
22	334	220	50	20	35.38
23	334	220	65	20	71.33
24	334	220	65	20	54.01
25	334	330	65	20	75.4
26	334	220	80	20	90.77
27	334	220	65	20	75.33
28	167	110	50	30	26.47
29	501	110	80	30	59.22
30	501	110	50	30	14.77

A quadratic polynomial equation is usually used to fit the experimental data (Cho & Zoh, 2007; Jalali & Sobati, 2017; Karami et al., 2017; Khodaei et al., 2016a, 2016b); therefore, a mathematical equation relating response to controllable factors (i.e. sonication time, temperature, H_2O_2/S molar ratio, and acetic acid/S molar ratio) is given by:

$$\begin{aligned}\text{DBT conversion (\%)} &= -213.5316155 - 0.0443497 \times \text{H}_2\text{O}_2/\text{S molar ratio} + 0.457430456 \\ &\times \text{Acetic acid/S molar ratio} + 6.468060916 \times \text{Temperature} \\ &- 2.365264985 \times \text{Sonication time} + 0.000170693 \times \text{H}_2\text{O}_2/\text{S molar ratio} \\ &\times \text{Acetic acid/S molar ratio} + 0.00079017 \times \text{H}_2\text{O}_2/\text{S molar ratio} \\ &\times \text{Temperature} + 0.000114147 \times \text{H}_2\text{O}_2/\text{S molar ratio} \times \text{Sonication time} \\ &+ 0.000460985 \times \text{Acetic acid/S molar ratio} \times \text{Temperature} \\ &+ 0.000590341 \times \text{Acetic acid/S molar ratio} \times \text{Sonication time} \\ &+ 0.031070833 \times \text{Temperature} \times \text{Sonication time} - 0.000115747 \\ &\times (\text{H}_2\text{O}_2/\text{S molar ratio})^2 - 0.000924634 \times (\text{Acetic acid/S molar ratio})^2 \\ &- 0.048346979 \times (\text{Temperature})^2 + 0.028919298 \times (\text{Sonication time})^2\end{aligned} \quad (3)$$

The sign and value of each of the coefficients show that the related parameter has a synergistic or antagonistic effect. Table 3 tabulates the analysis of variance (ANOVA) results of the correlation proposed by this study. In this correlation, the *F*-statistic or *F*-value of a factor is calculated as the mean square of that factor divided by the mean square of the residual. Generally speaking, in order to understand the interaction patterns between the parameters, the *F*-value and "Significance probability" or "*P*-value" can be employed. Needless to say, the smaller the *P*-value is and the greater the F-value is, the more substantial the associated variable becomes. To calculate the significance of a factor, the values of "P-value" were required to be checked. Here, if this value is less than 0.05, it can be understood that the model terms are significant, while values larger than 0.1 indicate the insignificance of the factors. From the *F*-value of the model (11.25), it can be implied that the model is significant. From the *F*-value listed in Table 3, it is evident that acetic acid/S molar ratio, temperature, and sonication time are the most significant parameters in the proposed correlation. It should be mentioned that temperature is the main factor affecting the DBT conversion. Moreover, according to the *F*-Value of "lack of fit" (see Table 3), it can be seen that the proposed model fairly well matches the data.

Table 3

Analysis of variance of the second order polynomial equation.

Source	**Sum of squares**	***df***	**Mean square**	***F*-value**	***P*-value (Prob > *F*)**
Model	16311.02	14	1165.02	11.25	<0.0001 Significant
A: H_2O_2/S molar ratio	466.14	1	466.14	4.5	0.0509
B: Acetic acid/S molar ratio	4859.67	1	4859.67	46.93	<0.0001
C: Temperature	5541.24	1	5541.24	53.52	<0.0001
D: Sonication time	1725.59	1	1725.59	16.67	0.0010
AB	157.31	1	157.31	1.52	0.2367
AC	62.69	1	62.69	0.61	0.4486
AD	0.58	1	0.58	0.006	0.9413
BC	9.26	1	9.26	0.089	0.7690
BD	6.75	1	6.75	0.065	0.8020

Source	Sum of squares	*df*	Mean square	*F*-value	*P*-value (Prob > *F*)	
CD	347.54	1	347.54	3.36	0.0869	
A^2	27.00	1	27.00	0.26	0.6170	
B^2	324.31	1	324.31	3.13	0.0971	
C^2	306.59	1	306.59	2.96	0.1051	
D^2	21.67	1	21.67	0.21	0.6539	
Residual	1553.12	15	103.54			
Lack of fit	758.08	10	75.81	0.48	0.8508	Not significant
Pure error	795.04	5	159.01			
Cor total[1]	17864.14	29				

[1] This row shows the amount of variation around the mean of the observations.

To see if the residuals followed a normal distribution and validated the experimental data, the analysis of normal probability plots was carried out. Figure 2 illustrates the normal probability plot of the residuals. It is obvious that the residuals follow a normal distribution because the points are almost located along a straight line. Both residuals and the predicted values are depicted in Figure 3, and it shows that the points are randomly distributed and located between -3 and +3, confirming that the model is both accurate and reliable. The plots of the predicted value along with the actual values are also presented in Figure 4. It can be seen that the experimental data are well predicted by the regression equation.

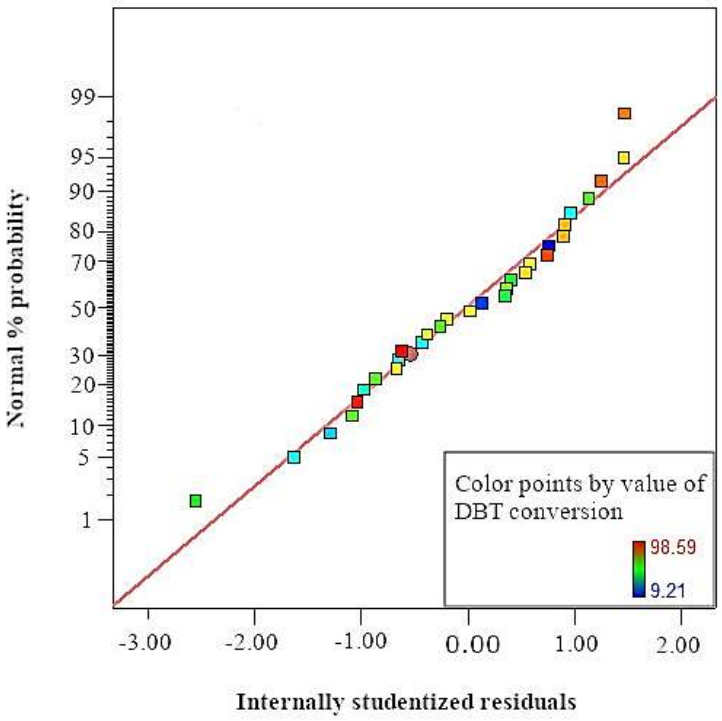

Figure 2

Normal probability plot of quadratic model fitted to the response data.

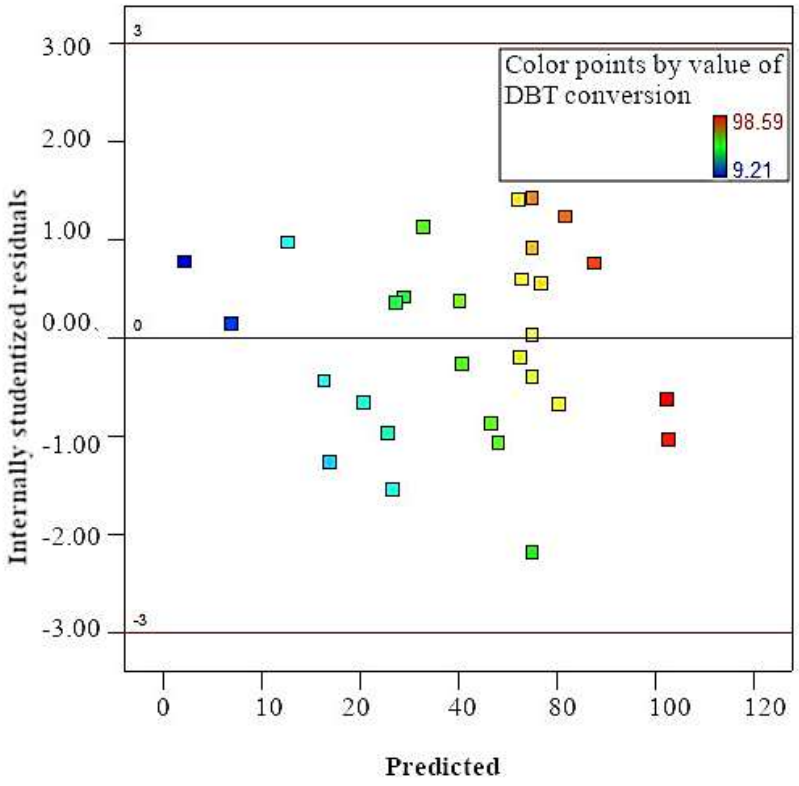

Figure 3

Residuals versus predicted values.

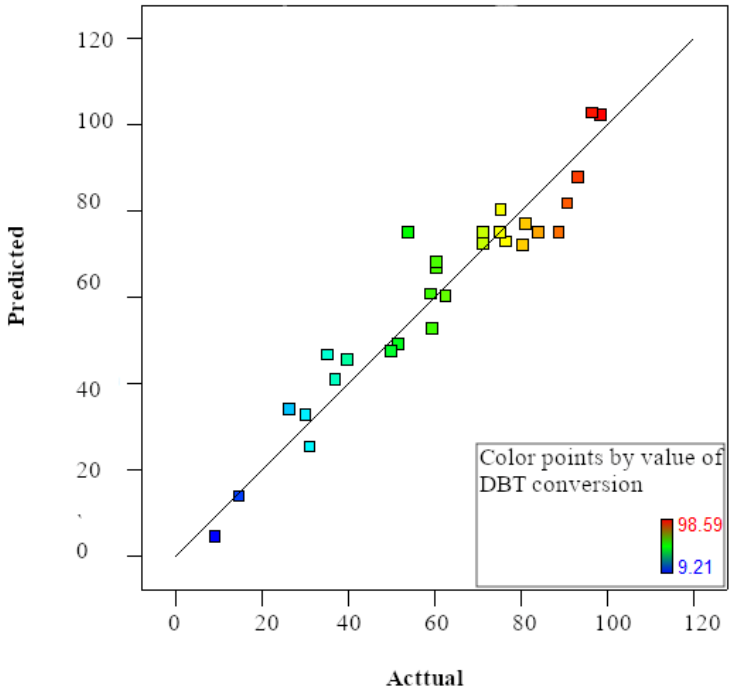

Figure 4

Predicted response versus actual response.

Furthermore, for the analysis of the interactions between the selected parameters (H_2O_2/S molar ratio, acetic acid/S molar ratio, temperature, and sonication time) and the DBT conversion, three-dimensional surface plots of the responses are illustrated in Figure 5. From Figure 5a, it can be seen that by increasing the H_2O_2/S molar ratio at a lower acetic acid/S molar ratio, the DBT conversion dropped; however, at higher acetic acid/S molar ratios, conversion first increased, then reached a maximum, and finally fell steadily. This can be due to an increase in the volume fraction of the aqueous phase. At the minimum molar ratio of acetic acid to sulfur, the dilution effect of the aqueous phase was strong enough to prevent an effective contact between the organic phase and the aqueous phase. It was observed that when the concentration of the acetic acid rose (at the maximum value of acetic acid/S molar ratio), the peroxyacetic acid concentration increased in the reaction medium at a lower concentration of hydrogen peroxide. After certain molar ratio of H_2O_2 to S, the reaction medium was diluted more because of the presence of aqueous phase, and the appropriate contact between both aqueous and organic phases finally decreased as the oxidation reactions continued. Figure 5b represents the interaction between temperature and H_2O_2/S molar ratio at a constant acetic acid/S molar ratio of 220 and a sonication time of 20 min. It is clear that the temperature had a great effect on the DBT conversion. By increasing the temperature at any constant H_2O_2/S molar ratios, the DBT conversion constantly enhanced. Moreover, the slope of DBT conversion versus temperature was higher at lower temperatures, which can be explained by the notion that the oxidation reactions are endothermic and proceed forwards by increasing temperature. However, at higher temperatures the slope is not so high, which is attributed to the degradation of hydrogen peroxide at higher temperatures. As a consequence, the concentration of hydroxyl radicals dropped. Figure 5c illustrates the synergistic effect of sonication time and H_2O_2/S molar ratio. As it can be seen, when the sonication time was extended from 10 min to 30 min, DBT conversion improved. Similarly, it can be seen that the conversion curve is steeper at high sonication times due to the reaction area expansion by the generation of more bubbles at higher sonication times. In addition, the interaction between the temperature and acetic acid/S molar ratio is depicted in Figure 5d, and Figure 5e displays the synergistic effect of sonication time and acetic acid/S molar ratio. It is evident that the sonication time had a positive effect on DBT conversion at both low and high molar ratios of acetic acid to sulfur. This can be explained by the fact that increasing the sonication time expands the interfacial area between the organic phase and the aqueous phase through the generation of microemulsions, so conversion improved. Figure 5f presents the interaction between sonication time and temperature. The maximum DBT conversion can be obtained at the maximum values of temperature and sonication time. It is worth mentioning that the slope of DBT conversion against temperature is higher at the maximum sonication time. In fact, when sonication time was extended, the bubble generation inside the reaction medium increased; thus, the interfacial area between the aqueous phase and the organic phase grew. In other words, it was seen that as soon as hydroxyl radicals were generated due to increasing temperature, they were consumed by the oxidation reaction.

3.2. Optimum conditions

The optimum operation point was obtained using response surface methodology by considering pair interactions among the parameters affected the DBT conversion. Accordingly, the DBT conversion was set to be maximum while H_2O_2/S molar ratio, acetic acid/S molar ratio, and sonication time were set at the minimum value and the other variables were kept in range. The optimum conditions are listed in Table 4. Under these conditions, a DBT conversion of 58.8% was achieved. It was also discovered that the maximum conversion reached 98.59% when H_2O_2/S molar ratio, acetic acid/S molar ratio, reaction temperature, and sonication time were set to 167, 330, 80 °C, and 30 min respectively.

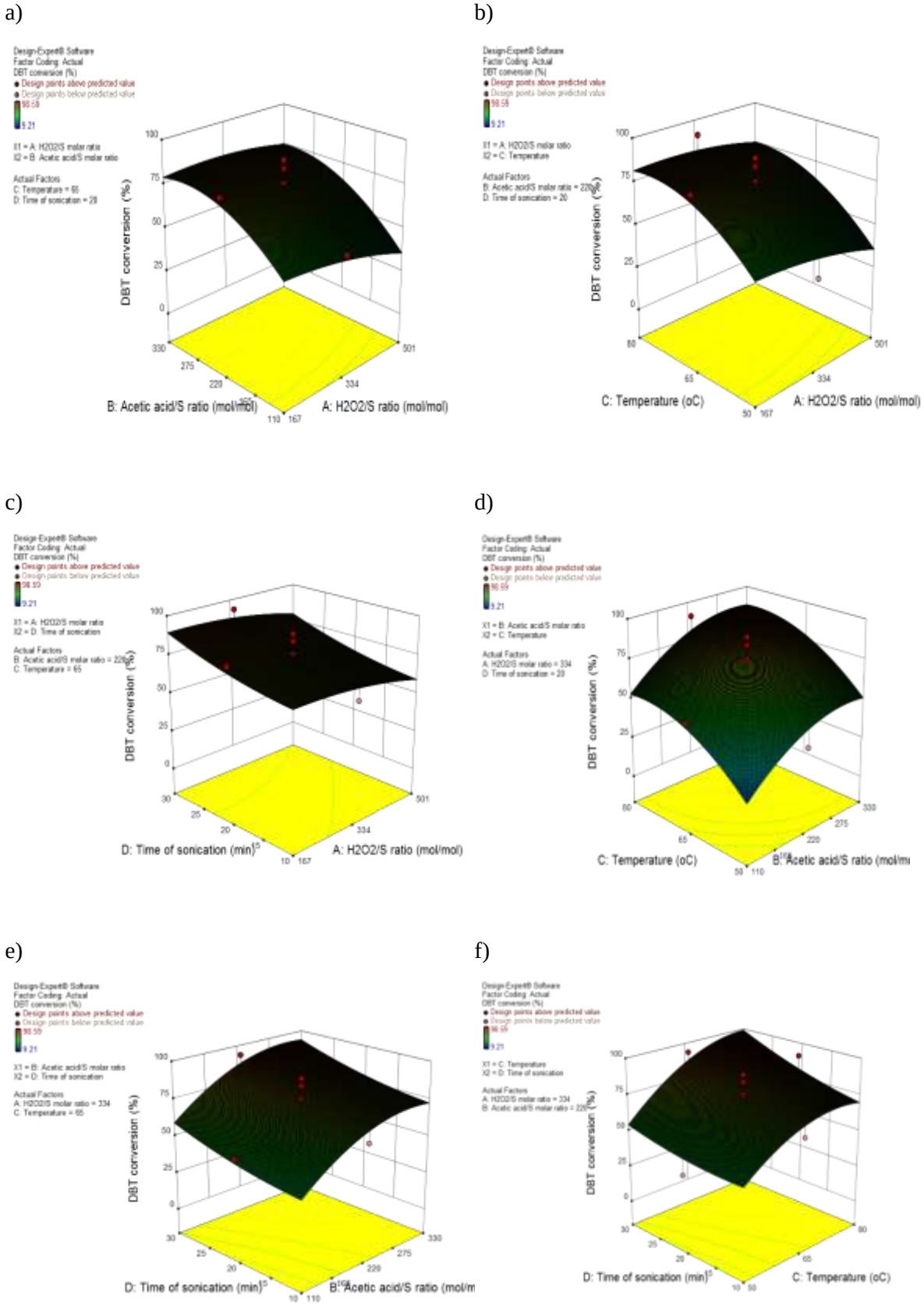

Figure 5

The effect of different parameters on DBT conversion.

Table 4

Optimum conditions.

Parameter	Value
H_2O_2/S (mol/mol)	167
Acetic acid/S (mol/mol)	142
Temperature (°C)	72
Sonication time (min)	10

3.3. Apparent kinetics of DBT oxidation reaction

The reaction kinetics is required for explaining the oxidation of DBT. A number of experiments were performed under the optimum conditions (H_2O_2/S=167 and acetic acid/S=142) to obtain the kinetic parameters of the oxidation of sulfur compounds. The variation of DBT conversion versus sonication time at four temperatures of 50, 60, 70, and 80 °C is plotted in Figure 6.

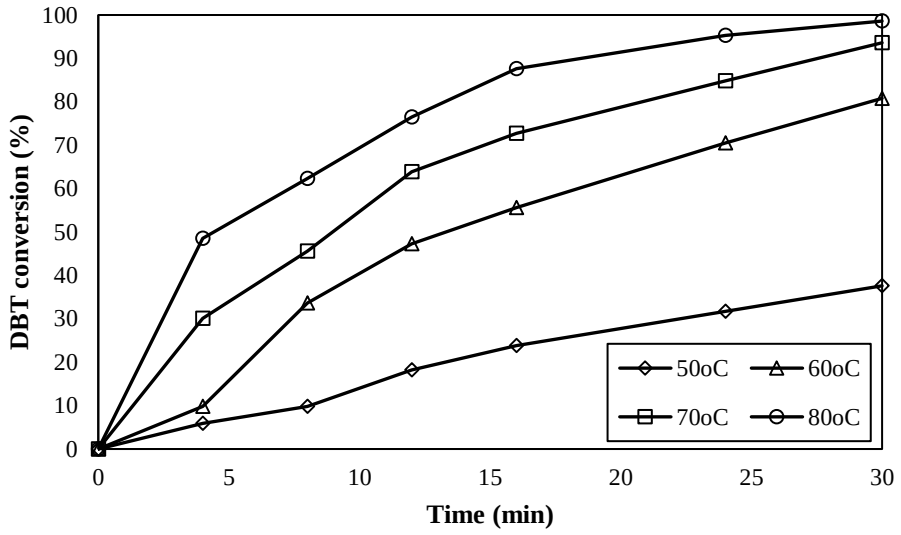

Figure 6

DBT conversion versus sonication time at different temperatures (H_2O_2/S=167, Acetic acid/S=142, and Power=800 W).

In order to investigate the kinetics, zero-order, pseudo-first order, and pseudo-second order reaction rates were utilized:

$$[C_{DBT}]_t = [C_{DBT}]_0 - kt \tag{4}$$

$$\ln\left(\frac{[C_{DBT}]_0}{[C_{DBT}]_t}\right) = kt \tag{5}$$

$$\frac{1}{[C_{DBT}]_t} = \frac{1}{[C_{DBT}]_0} - kt \tag{6}$$

where $[C_{DBT}]_0$ and $[C_{DBT}]_t$ are respectively the concentrations of DBT at the beginning point and at time *t*.

The R^2-value correlation coefficients of the curve fitting are tabulated in Table 5. One can conclude that the oxidation of DBT in the UAOD system follows the pseudo-first order kinetics model.

Table 5

R^2-value correlation coefficients of different kinetics models.

Kinetics model \ Temperature (°C)	50	60	70	80
Zero order	0.982401	0.933714	0.958143	0.890771
Pseudo-first order	0.995426	0.993946	0.971652	0.986026
Pseudo-second order	0.992151	0.942046	0.814906	0.744239

In addition, the linear curve of $\ln\left(\frac{[C_{DBT}]_0}{[C_{DBT}]_t}\right)$ versus time of the DBT oxidation reaction is illustrated in Figure 7. Using the slope of the curve, the reaction constant could be estimated to be 0.016118514, 0.056702548, 0.091041, and 0.13826861 min^{-1} at 50, 60, 70, and 80 °C respectively.

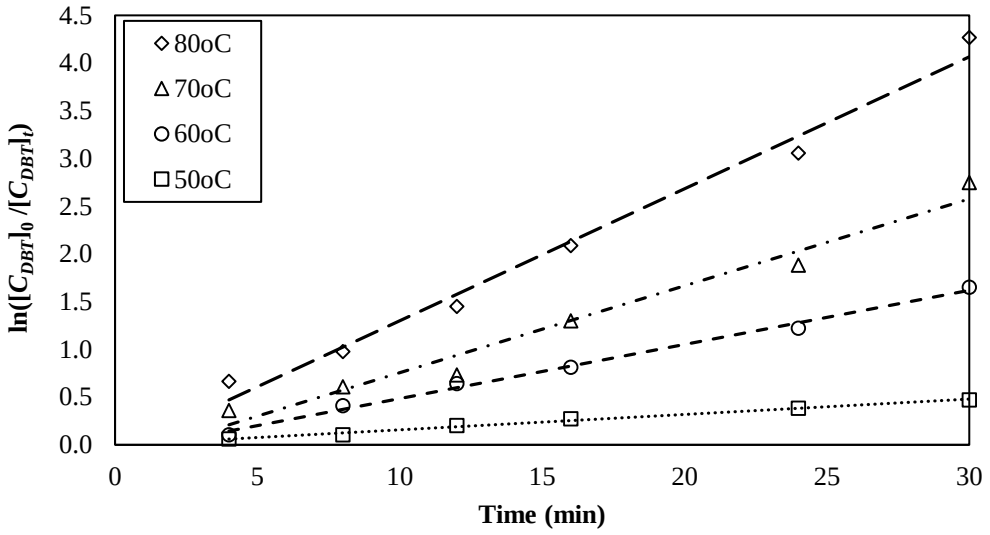

Figure 7

Pseudo-first order reaction rate equation.

Moreover, the activation energy of sulfur removal reaction can be calculated by the Arrhenius equation as follows:

$$k = Aexp\left(\frac{-E_a}{RT}\right) \tag{7}$$

where, A is pre-experimental factor, and E_a is the activation energy (kJ/mol); R, the gas constant, is considered to be 8.313 J/mol.K. k is the pseudo-first order constant. The logarithmic form of the equation is given by (Deshpande et al., 2005):

$$E_a = RT^2\frac{dlnk}{dT} \tag{8}$$

The plot of -ln(k) versus 1/T is also shown in Figure 8. From the slope of the curve, the E_a of the DBT oxidation reaction was calculated to be 66.05 kJ/mol.

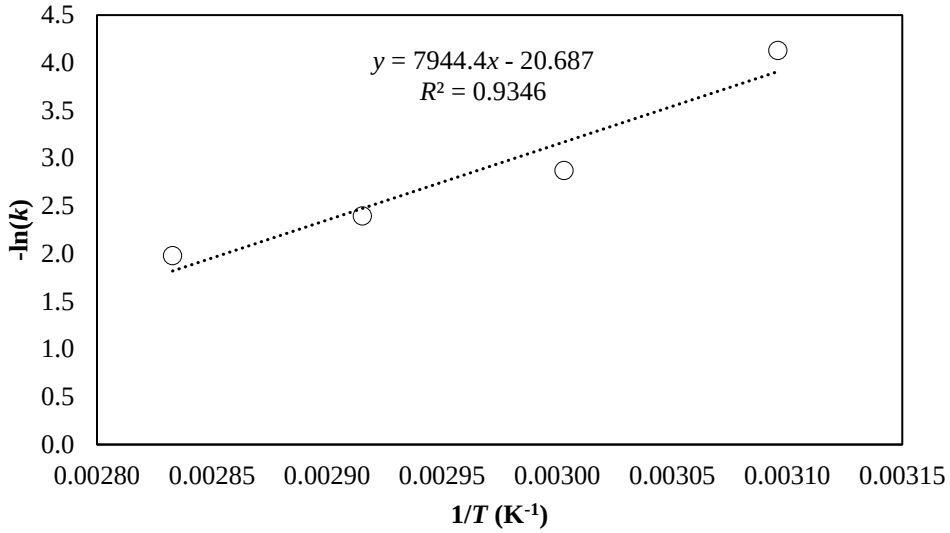

Figure 8

The plot of –ln(k) vs. 1/T.

4. Conclusions

The present study was an attempt to investigate the effects of operating parameters of a sonoreactor used for converting dibenzothiophene into sulfone in the ultrasound-assisted oxidative desulfurization process. For the purpose of optimizing DBT conversion via response surface method, this study utilized H_2O_2/S molar ratio, acetic acid/S molar ratio, temperature, and sonication time as the influencing parameters. The findings showed that temperature and acetic acid/S molar ratio were the most influencing parameters. It was also discovered that the conversion reached a maximum of 98.59% when H_2O_2/S molar ratio, acetic acid/S molar ratio, reaction temperature, and sonication time were respectively set at 167, 330, 80 °C, and 30 min. As a concluding remark, it was revealed that the reaction kinetics followed the pseudo-first order reaction rate model and that the activation energy of this reaction was 66.05 kJ/mol.

Nomenclature

ADS	Adsorptive desulfurization
BBD	Box-Behnken design
BDS	Biodesulfurization
BT	Benzothiophene
CCD	Central composite design
DBT	Dibenzothiophene
EDS	Extractive desulfurization
HDS	Hydrodesulfurization
NZVI	Nano zero valent iron
ODS	Oxidative desulfurization
phODS	photo-oxidative desulfurization
RSM	Response surface method
UAOD	Ultrasound-assisted oxidative desulfurization

References

Ahmadi, M., Anvaripour, B., Khosravi-Nikou, M. R., and Mohammadian, M., Selective Denitrogenation of Model Fuel Through Iron and Chromium Modified Microporous Materials (MSU-S), Journal of Environmental Chemical Engineering, Vol. 5, No. 1, p. 849–860, 2017, https://Doi.Org/10.1016/J.Jece.2017.01.007.

Ahmed, O. U., Mjalli, F. S., Wahaibi, T. Al., Al-Waheibi, Y. M., and Alnashef, I. M. Optimum Performance of Extractive Desulfurization of Liquid Fuels Using Phosphonium and Pyrrolidinium-based Ionic Liquids Optimum Performance of Extractive Desulfurization of Liquid Fuels Using Phosphonium and Pyrrolidinium-based Ionic Liquids, Industrial & Engineering Chemistry Research, Vol. 54, p. 6540–6550, 2015, https://Doi.Org/10.1021/Acs.Iecr.5b01187.

Akbari, A., Omidkhah, M., and Darian, J. T., Facilitated and Selective Oxidation of Thiophenic Sulfur Compounds Using MoO_x / Al_2O_3–H_2O_2 System under Ultrasonic Irradiation, Ultrasonics Sonochemistry, Vol. 23, p. 231–237, 2015, https://Doi.Org/10.1016/J.Ultsonch.2014.09.002.

Bachmann, R. T., Johnson, A. C., and Edyvean, R. G. J., Biotechnology in The Petroleum Industry: An Overview, International Biodeterioration & Biodegradation, Vol. 86, p. 225–237, 2014, https://Doi.Org/10.1016/J.Ibiod.2013.09.011.

Cho, I. and Zoh, K., Photocatalytic Degradation of Azo Dye (Reactive Red 120) in TiO_2/UV System : Optimization and Modeling Using A Response Surface Methodology (RSM) Based on the Central Composite Design, Dyes and Pigments, Vol. 75, p. 533–543, 2007, https://Doi.Org/10.1016/J.Dyepig.2006.06.041.

Dai, Y., Qi, Y., and Zhao, D., A Novel Technology for Desulfurization of FCC Diesel Fuels : Combination of Hydrogenation and Oxidation-assisted Ultrasound, Petroleum Science and Technology, Vol. 28, p. 146–154, 2010, https://Doi.Org/10.1080/10916460903058145.

Deshpande, A., Bassi, A., and Prakash, A., Ultrasound-assisted, Base-catalyzed Oxidation of 4,6-Dimethyldibenzothiophene in a Biphasic Diesel-acetonitrile System, Energy and Fuels, Vol. 19, No. 1, p. 28–34, 2005, https://Doi.Org/10.1021/Ef0340965.

Duarte, F. A., Mello, P. D. A., Bizzi, C. A., Nunes, M. A. G., Moreira, E. M., Alencar, M. S., Flores, É. M. M., Sulfur Removal from Hydrotreated Petroleum Fractions Using Ultrasound-assisted Oxidative Desulfurization Process, Fuel, Vol. 90, p. 2158–2164, 2011,https://Doi.Org/10.1016/J.Fuel.2011.01.030.

Ebrahimi, S. L., Khosravi-Nikou, M. R., and Hashemabadi, S. H. Sonoreactor Optimization for Ultrasound Assisted Oxidative Desulfurization of Liquid Hydrocarbon, Petroleum Science and Technology, Vol. 36, No 13, p. 959–965, 2018, https://Doi.Org/10.1080/10916466.2018.1458112.

Ja'fari, M., Ebrahimi, S. L., and Khosravi-Nikou, M. R., Ultrasound-assisted Oxidative Desulfurization and Denitrogenation of Liquid Hydrocarbon Fuels: A Critical Review. Ultrasonics Sonochemistry, Vol. 40 (Part A), p. 955–968, 2018, https://Doi.Org/https://Doi.Org/10.1016/J.Ultsonch.2017.09.002.

Ja'fari, M., Khosravi-Nikou, M. R., and Motavassel, M., Sulfur Removal of Hydrocarbon Fuels Using Oxidative Desulfurization Enhanced by Fenton Process, World Academy of Science, Engineering and Technology, Vol. 10, No. 12, p. 1455–1460, 2016.

Jalali, M. R. and Sobati, M. A., Intensification of Oxidative Desulfurization of Gas Oil by Ultrasound Irradiation : Optimization Using Box-behnken Design (BBD), Applied Thermal Engineering,

Vol. 111, p. 1158–1170, 2017, https://Doi.Org/10.1016/J.Applthermaleng.2016.10.015.

Jamei, M. R., Khosravi, M. R. and Anvaripour, B., Investigation of Ultrasonic Effect on Synthesis of Nano Zero Valent Iron Particles and Comparison with Conventional Method. Asia-Pacific Journal of Chemical Engineering, Vol. 8, p. 767–774, 2013, https://Doi.Org/10.1002/Apj.

Jamei, M. R., Khosravi, M. R., and Anvaripour, B., A Novel Ultrasound Assisted Method in Synthesis of NZVI Particles, Ultrasonics Sonochemistry, Vol. 21, No. 1, p.226–233, 2014, https://Doi.Org/10.1016/J.Ultsonch.2013.04.015.

Karami, E., Sobati, M. A., Khodaei, B., and Abdi, K., An Experimental Investigation on the Ultrasound-Assisted Oxidation of Benzothiophene in Model Fuel: Application of Response Surface Methodology, Applied Thermal Engineering, Vol. 118, p. 691-702, 2017, https://Doi.Org/10.1016/J.Applthermaleng.2017.03.028.

Khodaei, B., Sobati, M. A., and Shahhosseini, S., Optimization of Ultrasound-assisted Oxidative Desulfurization of High Sulfur Kerosene Using Response Surface Methodology (RSM), Clean Technologies and Environmental Policy, Vol. 18, p. 2677–2689, 2016, https://Doi.Org/10.1007/S10098-016-1186-Z.

Khodaei, B., Sobati, M. A., and Shahhosseini, S., Rapid Oxidation of Dibenzothiophene in Model Fuel Under Ultrasound Irradiation, Monatshefte Für Chemie-chemical Monthly, Vol. 148, p. 387–396, 2016, https://Doi.Org/10.1007/S00706-016-1801-Z.

Lu, M.-C., Biel, L. C. C., Wan, M.-W., De Leon, R., and Arco, S., The Oxidative Desulfurization of Fuels with a Transition Metal Catalyst: A Comparative Assessment of Different Mixing Techniques, International Journal of Green Energy, Vol. 11, No. 8, p. 833–848, 2014, https://Doi.Org/10.1080/15435075.2013.830260.

Margeta, D., Sertić-Bionda, K., and Foglar, L., Ultrasound Assisted Oxidative Desulfurization of Model Diesel Fuel. Applied Acoustics, Vol. 103, p. 202-206, 2016, https://Doi.Org/10.1016/J.Apacoust.2015.07.004.

Mohammadian, M., Ahmadi, M., and Khosravi Nikou, M. R., Adsorptive Desulfurization and Denitrogenation of Model Fuel by Mesoporous Adsorbents (MSU-S And Coo-MSU-S), Petroleum Science and Technology, Vol. 35, No. 6, p. 608–614, 2017, https://Doi.Org/10.1080/10916466.2016.1265562.

Mohammadian, M., Khosravi-Nikou, M. R., Shariati, A., and Aghajani, M. Model Fuel Desulfurization and Denitrogenation Using Copper and Cerium Modified Mesoporous Material (MSU-S) through Adsorption Process, Clean Technologies and Environmental Policy, Vol. 20, p. 95-112, 2018, https://Doi.Org/10.1007/S10098-017-1460-8.

Parvizian, F., Rahimi, M., and Azimi, N., Macro- and Micromixing Studies on a High Frequency Continuous Tubular Sonoreactor, Chemical Engineering & Processing: Process Intensification, Vol. 57–58, p. 8–15, 2012, https://Doi.Org/10.1016/J.Cep.2012.04.006.

Parvizian, F., Rahimi, M., Faryadi, M., and Alsairafi, A. A., Comparison between Mixing in Novel High Frequency Sonoreactor and Stirred Tank Reactor, Engineering Applications of Computational Fluid Mechanics, Vol. 6, No. 2, p. 295–306, 2012.

Rahimi, M., Shahhosseini, S., and Movahedirad, S., Continuous- flow Ultrasound Assisted Oxidative Desulfurization (UAOD) Process: An Efficient Diesel Treatment by Injection of the Aqueous Phase, Ultrasonics Sonochemistry, Vol. 39, p. 611–622, 2017.

Rashidi, S., Khosravi Nikou, M. R., and Anvaripour, B., Adsorptive Desulfurization and Denitrogenation of Model Fuel Using HPW and Nio-HPW Modified Aluminosilicate Mesostructures. Microporous and Mesoporous Materials, Vol. 211, p. 134–141, 2015, https://Doi.Org/10.1016/J.Micromeso.2015.02.041.

Rashidi, S., Khosravi Nikou, M. R., Anvaripour, B., and Hamoule, T., Removal of Sulfur and Nitrogen Compounds from Diesel Fuel Using MSU-S, Iranian Journal of Oil & Gas Science and Technology, Vol. 4, No. 1, p. 1–16, 2015.

Sahragard, H., Khosravi-Nikou, M. R., and Maddahi, M. H, An Optimization of Process Parameters for Deep Desulfurization of Model Fuel by ZSM-5/ZnO Photocatalyst Using Response Surface Method, Petroleum Science and Technology, Vol. 35, No. 19, p. 1879–1887, 2017, https://Doi.Org/10.1080/10916466.2017.1369113.

Sasanipour, J., Shariati, A., Aghajani, M., and Khosravi-Nikou, M., Dibenzothiophene Removal from Model Fuel Using an Acid Treated Activated Carbon, Petroleum Science and Technology, Vol. 35, No. 21, p. 1–8, 2017, https://Doi.Org/10.1080/10916466.2017.1381709.

Shayegan, Z., Razzaghi, M., Niaei, A., Salari, D., Tabar, M. T. S., and Akbari, A. N., Sulfur Removal of Gas Oil Using Ultrasound-assisted Catalytic Oxidative Process and Study of its Optimum Conditions, Korean Journal of Chemical Engineering, Vol. 30 ,No. 9, p. 1751–1759, 2013, https://Doi.Org/10.1007/S11814-013-0097-5.

Tang, Q., Lin, S., Cheng, Y., Liu, S., and Xiong, J., Ultrasound-assisted Oxidative Desulfurization of Bunker-C Oil Using Tert-butyl Hydroperoxide, Ultrasonics Sonochemistry, Vol. 20, No. 5, p. 1168–1175, 2013, https://Doi.Org/10.1016/J.Ultsonch.2013.02.002.

Te, M., Fairbridge, C., and Ring, Z., Oxidation Reactivities of Dibenzothiophenes in Polyoxometalate/H_2O_2 and Formic Acid/H_2O_2 Systems, Applied Catalysis A: General, Vol. 219, p. 267–280, 2001.

Wu, Z. and Ondruschka, B., Ultrasound-assisted Oxidative Desulfurization of Liquid Fuels and its Industrial Application, Ultrasonics Sonochemistry, Vol 17, No. 6, p. 1027–1032, 2010, https://Doi.Org/10.1016/J.Ultsonch.2009.11.005.